

Chandra X-ray observations of the stellar group near the Herbig Be star MWC 297

A revision of the X-ray properties of MWC 297

F. Damiani, G. Micela, and S. Sciortino

INAF - Osservatorio Astronomico di Palermo G.S.Vaiana, Piazza del Parlamento 1, 90134 Palermo, Italy
e-mail: damiani@astropa.unipa.it

Received 14 June 2005 / Accepted 11 October 2005

ABSTRACT

We present a *Chandra* ACIS-I X-ray observation of the region near the Herbig early-Be star MWC 297, where we detect a tight group of point X-ray sources. These are probably physically associated to MWC 297, because of their obvious clustering with respect to the more scattered field-source population. These data are compared to earlier ASCA data with much poorer spatial resolution, from which the detection of strong quiescent and flaring emission from MWC 297 itself was claimed. We argue that this star, contributing only 5% to the total X-ray emission of the group, was probably not the dominant contributor to the observed ASCA emission, while the X-ray brightest star in the group is a much better candidate. This is also supported by the spectral analysis of the *Chandra* data, with reference to the ASCA spectra. We conclude that none of the X-ray data available for MWC 297 justify the earlier claim of strong magnetic activity in this star. The X-ray emission of MWC 297 during the *Chandra* observation is even weaker than that found in other Herbig stars with the same spectral type, even accounting for its large line-of-sight absorption.

Key words. stars: early-type – stars: individual: MWC 297 – stars: emission-line, Be – stars: coronae – stars: pre-main sequence – X-rays: stars

1. Introduction

MWC 297 is a Herbig Be star, a more massive analogue of very young, pre-main-sequence (PMS) stars like T Tauri stars. It shows all “classical” features of the class, namely a B-type spectrum with strong emission lines, and is deeply embedded in a nebulous region (Herbig 1960). Indeed, it is one of the earliest-type stars in its class. Its spectral type was not defined in detail until recently, being its spectrum dominated by emission lines: the study of Finkenzeller & Mundt (1985) does not assign a spectral type, Hillenbrand et al. (1992) tabulate a type O9, while a dedicated study by Drew et al. (1997) concluded that this star is of type B1.5, with only half a subclass uncertainty. All these studies were made more difficult by the large visual extinction towards the star, whose estimates by various studies seem to converge towards the value $A_V = 8$. This is also the value derived by Drew et al. (1997), who moreover argue that the most likely distance of this star is 250 ± 50 pc, much nearer than previous estimates of about 500 pc (Cantó et al. 1984; Bergner et al. 1988).

As an early type star, the phenomena which can be expected from MWC 297 should be similar to those encountered in OB stars, and unlike those of late-type stars. It was therefore surprising that Hamaguchi et al. (2000, henceforth HTBK)

reported the detection of a large flare in an X-ray observation of this object, made with the ASCA satellite, since this type of variability is associated with magnetic-related activity, ordinarily found in stars later than mid-F, but disappearing for earlier-type stars, where surface convection is absent, and any dynamo-related magnetic activity should cease. Among Herbig Ae-Be stars, MWC 297 is the only star where such type of variability has been found in the ASCA survey of Hamaguchi et al. (2005), with the insignificant exception of TY CrA, which has a known later-type companion.

Herbig stars like MWC 297 are particularly interesting objects for studies of possible magnetic activity, since they are stars in a fast transition phase, between their formation and their settling on the main sequence, and some models (Siess et al. 2000) predict a transient subphotospheric convection zone, which might sustain magnetic activity for some time. This is indeed suggested by observations of optical/UV lines in some Herbig Ae stars (AB Aur, Praderie et al. 1986; HD 104237, Donati et al. 1997; HD 139614, Hubrig et al. 2004). Therefore, a further study of the X-ray emission of MWC 297 is made here, using archive data taken with the *Chandra* X-ray Observatory ACIS-I imaging spectrometer. This instrument has a roughly similar bandpass and effective

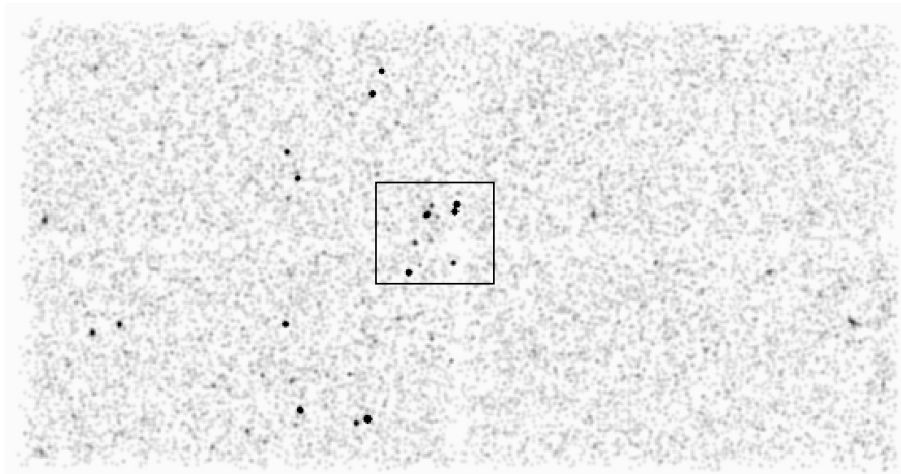


Fig. 1. *Chandra* ACIS-I image of the MWC 297 region, slightly smoothed to highlight the sources. The (windowed) field of view has a size of $16.9' \times 8.7'$. The outlined rectangle (of size $2.3' \times 2.0'$) contains MWC 297, and is zoomed in Fig. 2. The group of X-ray sources in this region was not resolved by ASCA. North is up and East to the left.

area as the (combined) ASCA SIS and GIS detectors but much better spatial resolution, of order of $0.5''$, while that of ASCA was of order of $3'$.

2. *Chandra* X-ray observation and source detection

MWC 297 was observed with the ACIS-I CCD imaging spectrometer onboard the *Chandra* X-ray Observatory on September 21–22, 2001. The exposure time was 37 330 s. A “windowed” observing mode was used, yielding a field of view (FOV) of $16.9' \times 8.7'$ (Fig. 1).

We have detected X-ray sources in the field using PWDetect, a wavelet-based detection algorithm developed at INAF-Osservatorio Astronomico di Palermo, and available as a *Chandra* contributed software¹; it inherits basic features of its previous ROSAT version, described in Damiani et al. (1997a,b). Using this method, we detected 27 point sources (with less than one expected spurious), listed in Table 1.

We have applied a Kolmogorov-Smirnov test for source variability, and we have found only one source (#1 in Table 1) with significant variability above 99% confidence level. This source is about 8 arcmin West of MWC 297 (the source at far right in Fig. 1), and even with the poorer ASCA spatial resolution could not have been confused with MWC 297 itself.

We also report in Table 1 two hardness ratios² (columns HR1 and HR2), each defined as $(H - S)/(H + S)$, where H and S are the source counts in two energy bands, here chosen as [1.3–2.5] and [0.3–1.3] keV for HR1, and [2.5–8.0] and [1.3–2.5] keV for HR2. HR1 describes roughly the low-energy cutoff caused by heavy absorption of soft X-rays, while a large value of HR2 is generally indicative of a high-energy component (high temperatures). Most X-ray sources in this

region have a large HR1, and are probably highly absorbed. A more detailed analysis is made in Sect. 4.

Our X-ray source #12 coincides closely with the position of MWC 297 (from the SIMBAD database), and a zoom of the ACIS image near the star is shown in Fig. 2a. The very good spatial resolution of *Chandra* is able to resolve the MWC 297 X-ray source from a neighboring one, only about 3 arcsec apart. The field shown in Fig. 2a is only $2.3' \times 2.0'$ in size, and therefore comparable to the ASCA PSF. The nine X-ray sources we detect in this region were merged into one when observed with ASCA. A proper comparison between these new data and the older ones from ASCA should involve the entire group of nine ACIS sources (henceforth called as “MWC 297 group”), not just the MWC 297 source. It turns out that MWC 297 is *not* the brightest X-ray source in its group: sources #5 and #6 are much brighter (they are the two sources in the upper-right quadrant of Fig. 2a). Table 2 lists the relative contributions to the total X-ray count rate among members of the MWC 297 group. Note that since some of the sources are underexposed (falling in inter-chip gaps, barely visible in Fig. 1) the actually detected counts do not scale with the same proportion, but the count rate accounts properly for this, yielding the “true” intensity of the sources.

The close spatial association of X-ray sources in the MWC 297 group (1/3 of all sources in the field, in 1/32 of the area) suggests that this group is a physical association, not a chance one. The existence of a small cluster of infrared objects around MWC 297 was already reported by Testi et al. (1998), and by Bica et al. (2003). Therefore, we may safely assume that all objects in the group have nearly the same age and distance as MWC 297, when trying to determine their nature.

3. X-ray source identification

To obtain some information on the nature of the detected sources, none of which (except for MWC 297) can be associated with objects in the SIMBAD database, we have searched the 2MASS catalog (Cutri et al. 2003) for possible identifications with infrared (IR) sources, within 4σ of the X-ray positions (with σ taken as the X-ray position error from Table 1). We have found 17 IR sources identified with an X-ray source,

¹ See http://www.astropa.unipa.it/progetti_ricerca/PWDetect/

² We selected the energy bands used to compute these hardness ratios in such a way as to maximize the average observed source counts in each band. Since these bands are not identical to those used in previous works, the values of HR1, HR2 in Table 1 should not be directly compared to those reported elsewhere for stars of similar type.

Table 1. X-ray sources detected in the ACIS-I image. The first six columns are the source number, its position with error, count rate with error, and exposure time. The last two columns are the X-ray hardness ratios, HR1 and HR2, as defined in the text.

X-ray No.	RA J2000.0	Dec J2000.0	Pos. Err. (")	Count rate (counts/ks)	Exp. time (ks)	HR1	HR2
1	18:27:06.00	-3:51:57.8	1.76	0.662 ± 0.249	25.582	0.391	-0.333
2	18:27:12.53	-3:50:58.6	1.87	0.384 ± 0.160	31.960	0.333	0.500
3	18:27:21.44	-3:50:47.5	0.76	0.232 ± 0.130	34.460	1.000	0.647
4	18:27:25.84	-3:49:05.0	0.32	0.158 ± 0.127	35.712	–	1.000
5	18:27:37.08	-3:49:39.1	0.29	5.044 ± 0.696	12.075	0.812	0.574
6	18:27:37.23	-3:49:47.0	0.22	3.328 ± 0.499	15.080	0.727	-0.369
7	18:27:37.36	-3:50:48.3	0.50	0.537 ± 0.238	18.213	1.000	0.900
8	18:27:39.11	-3:52:17.9	0.54	0.186 ± 0.094	36.659	1.000	0.600
9	18:27:39.11	-3:49:40.5	0.29	0.184 ± 0.116	36.794	1.000	-0.385
10	18:27:39.13	-3:46:11.3	0.50	0.224 ± 0.107	34.620	1.000	-0.333
11	18:27:39.35	-3:49:50.1	0.43	0.463 ± 0.168	36.801	0.250	-0.818
12	18:27:39.52	-3:49:52.5	0.40	0.658 ± 0.220	36.792	-0.500	0.565
13	18:27:40.03	-3:50:50.0	0.40	0.158 ± 0.082	37.243	0.500	-0.500
14	18:27:40.36	-3:50:23.4	0.29	0.469 ± 0.309	14.503	–	1.000
15	18:27:40.86	-3:50:59.3	0.29	1.103 ± 0.176	37.100	0.556	-0.400
16	18:27:43.01	-3:47:02.1	0.50	0.827 ± 0.153	35.108	0.727	0.356
17	18:27:43.73	-3:47:29.0	0.36	0.968 ± 0.278	35.389	0.463	-0.224
18	18:27:43.98	-3:53:50.4	0.32	0.167 ± 0.129	34.785	-0.333	-1.000
19	18:27:44.11	-3:53:51.3	0.36	2.258 ± 0.292	34.733	0.881	-0.403
20	18:27:45.01	-3:53:55.8	0.79	0.527 ± 0.180	34.529	1.000	-0.150
21	18:27:49.38	-3:53:40.7	0.47	1.053 ± 0.188	34.007	0.759	-0.259
22	18:27:49.60	-3:49:08.9	0.40	0.529 ± 0.181	35.019	1.000	0.111
23	18:27:50.44	-3:48:37.4	0.54	0.604 ± 0.196	34.648	0.000	0.143
24	18:27:50.58	-3:52:00.0	0.65	0.908 ± 0.180	34.890	1.000	0.095
25	18:27:52.35	-3:53:00.0	0.76	0.233 ± 0.114	33.729	1.000	0.714
26	18:28:03.60	-3:51:59.4	0.86	0.539 ± 0.225	30.495	1.000	0.730
27	18:28:05.71	-3:52:09.9	1.51	0.800 ± 0.252	30.308	-0.070	-0.111

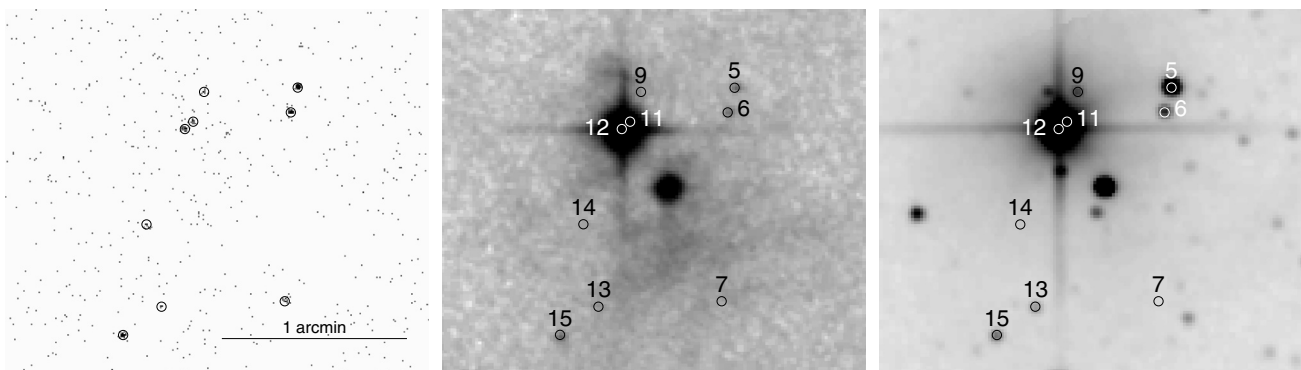


Fig. 2. a) Left: full-resolution zoom of ACIS X-ray image of the region near MWC 297, outlined in Fig. 1. Detected X-ray sources are indicated with circles. A segment shows the image scale. **b)** Middle: DSS red image of the same field shown in panel a). Circles indicate positions of X-ray detected sources, numbered as in Table 1. X-ray source #12 coincides with MWC 297. **c)** Right: K-band image of the same region, from 2MASS, with X-ray detections indicated.

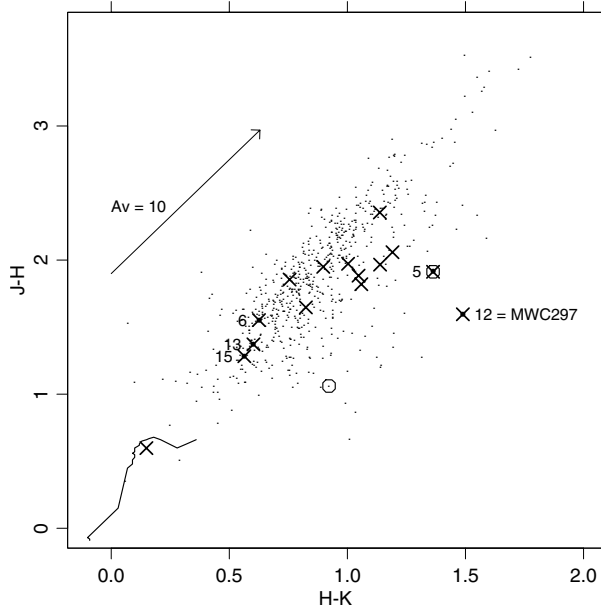
without ambiguous cases (Table 3). In the MWC 297 group, only 5 X-ray sources have an IR identification. The two brightest X-ray sources in the group, #5 and #6, are both identified. Although no optical catalog of stars in this region exists, we have compared our X-ray source positions with the DSS red image (see Fig. 2b): both sources #5 and #6 have a faint

optical counterpart. Figure 2c compares the X-ray source positions with the 2MASS K-band image, and shows that X-ray source #5 is indeed a bright object in the IR.

The nature of the sources with an IR identification can be studied using IR color-color and color-magnitude diagrams. A ($J-H$, $H-K$) diagram is shown in Fig. 3. X-ray detected objects

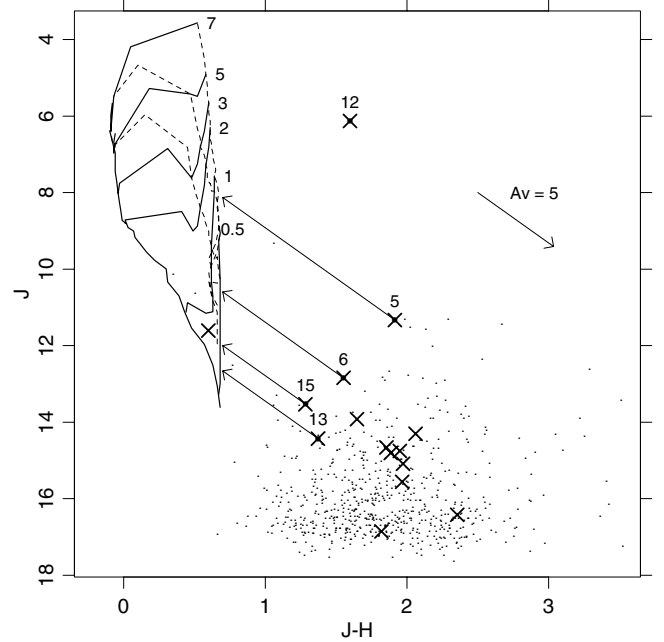
Table 2. Percentages of contribution from individual ACIS X-ray sources in the MWC 297 group to the total ASCA X-ray source.

X-ray No.	Contrib. (%)
5	42.2
6	27.9
7	4.5
9	1.5
11	3.9
12 (MWC 297)	5.5
13	1.3
14	3.9
15	9.2

**Fig. 3.** A $(J-H, H-K)$ color-color diagram of objects in the ACIS FOV. The locus of main-sequence stellar colors is shown by a solid line, and the arrow is the reddening vector for $A_V = 10$ (according to Rieke & Lebofsky 1985). X's are detected X-ray sources, among which those falling in the MWC 297 group (i.e., shown in Fig. 2) are numbered. Circles indicate objects with significant ($>3\sigma$) K -band excess with respect to normal colors.

are indicated with X's, and all of them but one (source #1, the only variable source) have IR colors indicative of large reddening ($A_V \sim 5-15$): they are either embedded in the same cloud as MWC 297 (as already argued for objects in the MWC 297 group), or they are background objects. As is already known, the IR spectrum of MWC 297 shows very large non-stellar excesses, as its very red $H-K$ color shows, compared to normal reddened stellar colors (solid line). Two other IR objects in the field show significant ($>3\sigma$) color excesses³ (affecting mostly the longer-wavelength K band), typical of young

³ In the $(J-H, H-K)$ diagram of Fig. 3, a few other IR objects fall redward of the reddened main-sequence colors, but the deviation is not significant above 3σ according to published errors in the 2MASS photometry.

**Fig. 4.** A $(J, J-H)$ color-magnitude diagram of objects in the ACIS FOV. Symbols are as in Fig. 3. In addition to the ZAMS, are also shown evolutionary tracks (solid) for various masses (as indicated), and isochrones for ages of 0.1, 0.3, and 1 Myr (dashed). The dereddened positions of X-ray sources in the MWC 297 group are indicated with arrows, assuming an intrinsic color $(J-H)_0 = 0.7$.

PMS stars: one is the bright object near the center of Figs. 2b and 2c, not detected in X-rays; the other is the brightest X-ray source (#5) in the MWC 297 group. The position of object #5 in the $(J-H, H-K)$ diagram suggests also a much larger extinction than all other IR-detected objects in the group (#6, #13 and #15, numbered in Fig. 3), except for MWC 297 itself.

Figure 4 is a $(J, J-H)$ color-magnitude diagram of the same objects, where evolutionary tracks with isochrones (from Siess et al. 2000) and the ZAMS (at a distance of 250 pc, Drew et al. 1997) are also plotted for reference. The plotted isochrones are for ages of 0.1, 0.3, and 1 Myr, while masses for the evolutionary tracks are indicated in the figure. We have chosen this color-magnitude diagram, making no use of the K band, to minimize the displacement (other than due to reddening) caused by non-stellar emission excesses, which affect mostly the longer wavelengths. Therefore, we may with some confidence de-redden the observed magnitudes and colors, by assuming normal stellar colors. This can be done meaningfully only for objects in the MWC 297 group, which we have argued are likely to lie all at the same distance as MWC 297. Under this assumption, we observe that all these objects (indicated by numbers in Fig. 4) are much fainter even in the IR than MWC 297, and their positions in the diagram suggest lower-mass stars than MWC 297 itself. We thus deredden their J magnitude assuming that their intrinsic color is $(J-H)_0 = 0.7$. This brings their positions in the $(J, J-H)$ diagram close to the expected locus of low-mass stars at ages of 0.1–0.3 Myr, consistently with our previous argument that these stars are coeval with the very young MWC 297. In particular, it is found that source #5 is a star of about $1 M_\odot$, while other X-ray sources in

Table 3. Identifications of X-ray sources with 2MASS infrared objects.

X-ray No.	2MASS name	Offset (")	<i>J</i>	<i>H</i>	<i>K</i>	Other id.
1	18270594-035157	0.88	11.605	11.007	10.857	
2	–	–	–	–	–	
3	–	–	–	–	–	
4	–	–	–	–	–	
5	18273709-034938	0.56	11.329	9.415	8.052	
6	18273723-034946	0.43	12.842	11.290	10.664	
7	–	–	–	–	–	
8	18273917-035218	1.35	16.853	15.033	13.974	
9	–	–	–	–	–	
10	18273914-034611	0.33	15.084	13.112	12.109	
11	–	–	–	–	–	
12	18273952-034952	0.45	6.127	4.53 ^a	3.041	MWC 297
13	18274002-035050	0.11	14.428	13.056	12.454	
14	–	–	–	–	–	
15	18274086-035059	0.12	13.530	12.247	11.683	
16	–	–	–	–	–	
17	18274372-034728	0.15	14.754	12.804	11.906	
18	–	–	–	–	–	
19	18274408-035351	0.50	13.996	–	–	
20	18274498-035355	0.44	14.662	12.807	12.052	
21	18274937-035340	0.32	13.924	12.277	11.453	
22	18274958-034908	0.29	–	15.061	13.356	
23	18275043-034837	0.26	14.805	12.920	11.873	
24	18275056-035200	0.23	14.301	12.241	11.050	
25	18275231-035300	0.68	16.423	14.068	12.931	
26	–	–	–	–	–	
27	18280564-035211	1.67	15.560	13.594	12.455	

^a MWC 297: *H* magnitude from Hillenbrand et al. (1992).

the MWC 297 group are stars of much lower mass ($\leq 0.3 M_{\odot}$). This very young, relatively bright, late-type star is expected to have a strong X-ray emission (up to $L_X \sim 10^{31}$ erg/s, e.g. Flaccomio et al. 2003), which justifies why it is found as the brightest source in the group.

4. X-ray luminosities and spectra, and comparison with ASCA data

We examine here the X-ray luminosities and spectra of our ACIS sources, comparing them with the analysis of ASCA data by HTBK. We recall that HTBK modeled the ASCA source (during the quiescent phase) as a single-temperature Raymond thermal spectrum, with absorption $N_H = 2.6(2.0\text{--}3.3) \times 10^{22}$ cm⁻² and temperature $kT = 2.7(2.1\text{--}4.1)$ keV ($\log T = 7.50(7.39\text{--}7.68)$ K); the metal abundance was poorly constrained (in the range 0.26–4.5), and compatible with solar abundance. The source luminosity (in the band 0.4–10 keV) was computed assuming a distance of 450 pc, and scaling it down to the revised value (250 pc) it becomes $L_X = 2.53(2.44\text{--}2.59) \times 10^{31}$ erg/s.

The conversion between ASCA and *Chandra* ACIS count rates depends very weakly on the detailed spectral parameters, in the range of interest: in the entire range of N_H and kT given by HTBK the conversion factor varies at most by 2.6%, as can

be derived using PIMMS⁴. The ASCA total (2 SIS + 2 GIS) quiescent count rate was reported by HTBK to be 0.023 cts/s, which again with PIMMS is seen to correspond to a one-SIS count rate of 0.00533 cts/s, and to an ACIS-I count rate of 0.01663 cts/s. We remind that this corresponds to the *entire MWC 297 group* (unresolved by ASCA), not to MWC 297 individually. The sum of ACIS count rates of sources in the group is 0.0119 cts/s, or 71.8% of the value predicted from ASCA data. The small difference can be ascribed to intrinsic stellar variability of the bright late-type sources #5 and #6, and also perhaps to residual uncertainties in the cross-calibration between ASCA and *Chandra* effective areas. Our conclusion is that *there is no substantial difference between the level of quiescent emission between the ASCA and the Chandra observations*.

This suggests that the relative contributions to the total group X-ray emission, even during the ASCA observation, should have not varied much with respect to the values found during the *Chandra* observation, reported in Table 2. Even if the “missing” 28% of the ASCA-predicted ACIS count rate were entirely due to a fading of MWC 297 during the *Chandra* observation (by a factor of 6) with respect to the ASCA one, this would raise the contribution of MWC 297 to the total count rate of the group only up to 33.5%, still less than source #5.

⁴ Portable Interactive Multi-Mission Simulator, <http://asc.harvard.edu/toolkit/pimms.jsp>

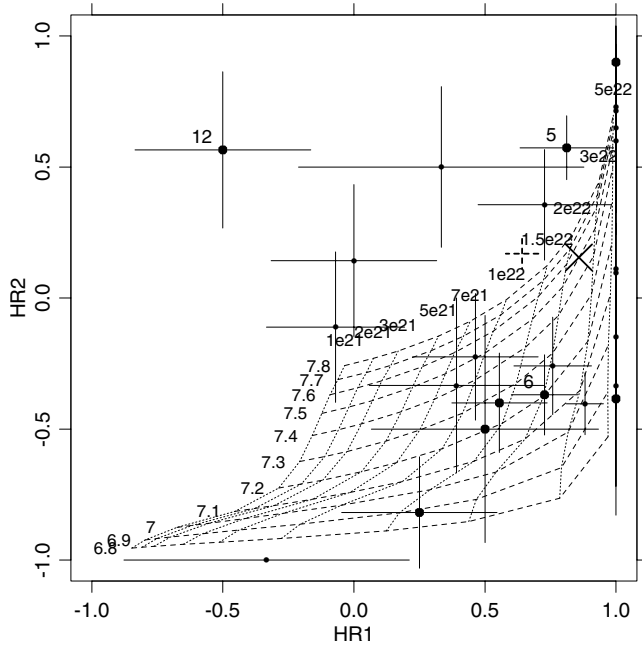


Fig. 5. Diagram of X-ray hardness ratios ($HR1$, $HR2$), for all sources in the ACIS FOV, with error bars. Sources in the MWC 297 group are indicated by filled dots, among which we label with numbers the strongest two sources (X-ray #5 and #6), and MWC 297 (X-ray #12). The dashed error bars indicate the combined (ACIS) hardness ratios of the whole MWC 297 group. The dotted-dashed grid indicates predicted hardness ratios for single-temperature Raymond X-ray spectra, for various temperatures ($\log T = 6.8\text{--}7.8$ K), and absorbing column densities ($N_H = 1 \times 10^{21}\text{--}5 \times 10^{22}$ cm $^{-2}$), as labeled. The thick X symbol corresponds to the predicted position according to the ASCA spectral parameters.

This latter source contributes 42.2% to the group count rate. Taking this percentage of the ASCA-derived luminosity yields an X-ray luminosity $L_X = 1.07 \times 10^{31}$ erg/s, perfectly plausible for a very young PMS solar-mass star (Flaccomio et al. 2003). Even the temperature of the X-ray source inferred from ASCA data by HTBK (2.7 keV) is well in the expected range for such a star. Therefore, all indications provided by the new *Chandra* data converge to a picture where the quiescent “MWC 297” ASCA source was in fact *not* dominated by the emission by MWC 297 itself, but by the neighboring source #5, an X-ray bright low-mass star.

Strengthening this view is the fact that the position itself of the ASCA source is much closer to source #5 (and #6) than to MWC 297 itself (see Hamaguchi et al. 2005, Table 5, and Fig. 8).

We gain additional useful information from considering the ACIS CCD X-ray spectra. All sources in the MWC 297 group are detected with a small number (≤ 60) of X-ray counts, and a detailed spectral analysis is not possible. We have nevertheless studied the X-ray hardness ratios, defined in Sect. 2. Figure 5 shows a ($HR1$, $HR2$) diagram of all ACIS sources in the field, among which those in the MWC 297 group are indicated with big dots. Most of these latter sources are well compatible with highly absorbed, moderately hot X-ray emission. The location of source #5 is indicative of hotter emitting plasma, and higher

absorption, in agreement with its being more X-ray active, and more absorbed (Sect. 3), than all other sources in the group. Finally, MWC 297 (source #12) occupies a different location (by more than 3σ) than all other sources in the group, indicative of a distinctly different X-ray spectral shape. In particular, its two hardness ratios suggest on one hand a soft source (despite the strong absorption, cutting out softer photons), on the other a hard-X-ray tail. The possible significance of this will be discussed below. The combined X-ray emission of all sources in the group is characterized by hardness ratios shown by the dashed error bars in Fig. 5. The predicted position of the same “group” X-ray source, as derived from the ASCA parameters as found by HTBK, is marked with an “X” symbol, and it falls near to the combined ACIS sources, demonstrating that the spectral parameters of the observed emission have not changed much between the *Chandra* and ASCA observations. Not surprisingly the “ASCA” source falls nearer to source #5 than to any other individual source in the group, again confirming that this source was dominating the ASCA-detected emission studied by HTBK.

The intrinsic X-ray spectrum (and luminosity) of MWC 297 cannot be determined from the ACIS data, because of the small number of detected counts. We can only examine whether it is compatible with the same model used for better studied Herbig Be stars, as similar as possible to MWC 297. A good “template” star may be HD 200775, of type B2.5e, a bright X-ray source already detected using *Einstein* (Damiani et al. 1994a) and ROSAT (Damiani et al. 1994b), and whose ASCA X-ray spectrum was studied in detail by Hamaguchi et al. (2005). Despite being farther (600 pc, Hillenbrand et al. 1992; or 430 pc from Hipparcos data, van den Ancker et al. 1997) than MWC 297, it is less absorbed. The ASCA X-ray spectrum of HD 200775 was modeled by Hamaguchi et al. (2005) with two thermal components, at 0.5 and 2.8 keV, with an emission measure of the high-temperature component one tenth that of the low-temperature component. We have taken this model, added an absorption $N_H = 1.78 \times 10^{22}$ cm $^{-2}$ (corresponding to $A_V = 8$, Gorenstein 1975) appropriate to MWC 297, and have let the total normalization to vary, keeping fixed the emission-measure ratio between components. The “fit” thus made was good ($\chi^2/\text{d.o.f.} = 0.44/2$), and the intrinsic source flux of MWC 297 according to this model is $f_X = 7.18 \times 10^{-14}$ erg/cm 2 /s, corresponding to a luminosity $L_X = 5.37 \times 10^{29}$ erg/s. Although we accounted for the higher absorption towards MWC 297, this X-ray luminosity is much lower than that of HD 200775. This latter was derived as $\log L_X = 31.63$ (erg/s) (Damiani et al. 1994a, down-scaled to the new Hipparcos distance), and as $\log L_X = 32.1$ (erg/s) (Hamaguchi et al. 2005, computed over a wider band, up to 10 keV).

5. Discussion and conclusions

In the previous sections we have presented a large body of evidences that most of the quiescent X-ray emission detected with ASCA by HTBK should be ascribed not to MWC 297, but to our ACIS sources #5 and #6, likely uncatalogued young low-mass stars. MWC 297 can account for only 5.5% of the

emission detected with ASCA. The most interesting question is however which star was the source of the powerful flare observed during the second ASCA observation studied by HTBK: they assigned this emission to MWC 297, and this was taken as an unprecedented detection of solar-type X-ray variability in an early-type star, to explain which they invoked a previously unsuspected magnetic activity.

In the ACIS data, we already noted that no X-ray source in the MWC 297 group exhibited significant variability, and this despite that the *Chandra* observation was longer (37.3 ks) than the ASCA observation (27.6 ks, in three segments). Evidently, such powerful events are rare. While, on the basis of previous knowledge, a magnetic flare in an early-type star is an extremely unlikely event, we may ask whether the same phenomenon, with the observed characteristics, can be more likely ascribed to other X-ray stars in the same group, and especially the brightest source, #5. We note first that the reduced distance with respect to that adopted by HTBK implies that the flare peak luminosity reduces to $L_X^{\text{peak}} = 1.39 \times 10^{32}$ erg/s. This is indeed a powerful flare, but not outside the known range of such events as observed in low-mass PMS stars: for example, Tsuboi et al. (1998) have observed with ASCA a giant flare from the low-mass PMS star V773 Tau, with peak X-ray luminosity around $L_X^{\text{peak}} = 10^{33}$ erg/s. Restricting ourselves to solar-mass PMS stars (i.e., what our source #5 appears to be), Wolk et al. (2005) have found a flare event with peak X-ray luminosity above $L_X^{\text{peak}} = 10^{32}$ erg/s in 1 out of 28 solar mass stars, observed for 850 ks as part of the Chandra Orion Ultradeep Project (COUP; Getman et al. 2005). The ASCA-derived temperature of the “MWC 297” flare (6.7 keV) is smaller than the temperature of the V773 Tau flare, and is within the range of Orion solar-mass stars in the COUP flare sample. The total released energy during the “MWC297” flare (again scaled to the lower distance with respect to HTBK) is 8.33×10^{36} erg, a value exceeded by 5/28 stars in the Wolk et al. (2005) sample.

We add that assigning the flare to MWC 297 would imply a flare-to-quiescent luminosity ratio >250 , a rather extreme value even for very active low-mass stars. Assigning it to source #5 yields instead a flare-to-quiescent ratio of 13, again well in the range found by Wolk et al. (2005). Therefore, there are sufficient reasons to suspect that the flare found by HTBK from the MWC 297 group was actually originated from source #5, not from MWC 297 itself. This picture stays within the boundaries of current knowledge of X-ray emission from PMS stars, without invoking hardly-explained coronal activity in an early-type star. We conclude that *there is no compelling evidence that the ASCA-detected flare was originated from MWC 297*.

HTBK did discuss the possibility that the X-ray emission they were observing could come from one or more lower-mass stars, but dismiss this hypothesis. Part of their reasoning stems from the large assigned X-ray luminosities, which resulted from their adopted distance value of 450 pc. With the new distance, X-ray luminosities are well compatible with low-mass coronal source(s). An assumption is made by HTBK, that any neighboring lower-mass star, at the age $\sim 10^5$ yr, must be considered as a protostar, with too low X-ray emission level. However, protostars are, almost by definition, deeply embedded, optically invisible objects, and our Fig. 2b shows that most

of our ACIS sources in the MWC 297 group (in particular our sources #5 and #6) *are* optically visible, and are thus to be regarded as low-mass PMS stars, with commonly found strong X-ray emission, both quiescent and flaring.

Regarding the true nature of the weak ACIS X-ray source identified by us with MWC 297, its luminosity is much lower than that of HD 200775, by a factor ~ 200 , despite the two stars have a similar spectral type. The most important differences between them reside probably in their circumstellar environments. MWC 297 has an extremely strong and variable $H\alpha$ emission, with equivalent width (*EW*) reaching up to 650 Å (Drew et al. 1997), while a lower value (but still very high) of 133 Å was reported by Finkenzeller & Mundt (1984). For comparison, the $H\alpha$ *EW* of HD 200775 was reported to vary between 55–110 Å by Pogodin et al. (2004). Therefore, the very energetic circumstellar phenomena which appear to take place around MWC 297, more powerful than those around HD 200775, seem to reduce rather than enhance X-ray emission, contrary to expectations of a wind-generated X-ray emission (suggested by Damiani et al. 1994a). The nature of the weak X-ray emission of MWC 297 is not elucidated by this comparison. It should be however noted that the data for HD 200775 come from low spatial-resolution instruments, while new *Chandra* data for this star are not available; these latter might well change our knowledge of the X-ray emission of HD 200775 as well.

A possibility worth investigation, which would explain the increasing X-ray luminosity of Herbig Ae/Be stars (observed at low-spatial resolution) was found to increase towards the optically brighter stars (Damiani et al. 1994a) is that these latter are surrounded by richer (and likely younger) groups of lower-mass objects (Testi et al. 1999), probable strong X-ray sources themselves. This fact was recognized *after* the early X-ray observations of these stars, and has apparently never taken properly into account in the interpretation of X-ray data on Herbig stars taken at low spatial resolution (e.g. with *Einstein* or ASCA). The much higher spatial resolution attained by *Chandra* would provide a test of this alternative. Unfortunately, only a handful Herbig stars have already been observed with *Chandra*.

The large value of HR2 (hard spectrum) found in our ACIS MWC 297 source is in qualitative agreement with the result found on other Herbig stars from ASCA data (Skinner & Yamauchi 1996; Hamaguchi et al. 2005), and more recently from *Chandra* and *XMM-Newton* data (Giardino et al. 2004; Skinner et al. 2004) of the existence of a hot component in Herbig stars’ X-ray spectra, with $kT > 1\text{--}1.5$ keV. As already noted, this is suggestive (but not conclusive) evidence of magnetically-related X-ray activity. In many of the observed cases it cannot be ruled out that this emission comes from late-type companions. Another possible scenario might be that proposed for the O star θ^1 Ori C by Gagné et al. (2005), where the observed properties of X-ray emission (including a higher temperature than commonly found in early-type stars) are well explained by a “magnetically channeled wind shock mechanism”.

We note that although the ASCA flare from MWC 297 probably never existed, another Herbig star

(V892 Tau = Elias 3-1) was observed to flare in X-rays by Giardino et al. (2004), and this poses again a problem to explain solar-like coronal activity in these stars with at most very shallow convective layers. Even this detection was recently challenged by Smith et al. (2005), who found a close companion (distinct from the already known companion V892 Tau NE, not the flare source of Giardino et al. 2004), at 50 mas from the Herbig star, and therefore unresolvable even with *Chandra*. This is probably a late-type star, good candidate as the flare source. An unambiguous detection of X-ray variability of magnetic origin in an Herbig Ae/Be star, not explainable as emission from a late-type companion, is probably still not available.

Acknowledgements. We acknowledge support from Italian MIUR. This study has made use of the 2MASS data, and of the SIMBAD database, operated at CDS, Strasbourg. We also thank the referee, Dr. S. J. Wolk, for useful comments on the manuscript.

Note added in proof After acceptance of this manuscript, we learned that similar results on the X-ray emission of MWC 297 had independently been obtained by Vink et al. (2005) and that this work had already been accepted for publication in A&A. Thus, our conclusions support those of the earlier-published work of Vink et al.

References

- Bergner, Y. K., Kozlov, V. P., Krivtsov, A. A., et al. 1988, *Astrophysics*, 28, 313
- Bica, E., Dutra, C. M., & Barbuy, B. 2003, *A&A*, 397, 177
- Cantó, J., Rodríguez, L. F., Calvet, N., & Levreault, R. M. 1984, *ApJ*, 282, 631
- Cutri, R. M., et al. 2003, Explanatory Supplement to the 2MASS All Sky Data Release, <http://www.ipac.caltech.edu/2mass/releases/allsky/doc/explsup.html>
- Damiani, F., Micela, G., Sciortino, S., & Harnden, F. R. 1994a, *ApJ*, 436, 807
- Damiani, F., Micela, G., & Sciortino, S. 1994b, The Nature and Evolutionary Status of Herbig Ae/Be Stars, ASP Conf. Ser., 62, 301
- Damiani, F., Maggio, A., Micela, G., & Sciortino, S. 1997a, *ApJ*, 483, 350
- Damiani, F., Maggio, A., Micela, G., & Sciortino, S. 1997b, *ApJ*, 483, 370
- Donati, J.-F., Semel, M., Carter, B. D., Rees, D. E., & Collier Cameron, A. 1997, *MNRAS*, 291, 658
- Drew, J. E., Busfield, G., Hoare, M. G., et al. 1997, *MNRAS*, 286, 538
- Finkenzeller, U., & Mundt, R. 1984, *A&AS*, 55, 109
- Flaccomio, E., Damiani, F., Micela, G., et al. 2003, *ApJ*, 582, 398
- Gagné, M., Oksala, M. E., Cohen, D. H., et al. 2005 [arXiv:astro-ph/0504296]
- Getman, K. V., Flaccomio, E., Broos, P. S., et al. 2005, *ApJS*, 160, 319
- Giardino, G., Favata, F., Micela, G., & Reale, F. 2004, *A&A*, 413, 669
- Gorenstein, P. 1975, *ApJ*, 198, 95
- Hamaguchi, K., Terada, H., Bamba, A., & Koyama, K. 2000, *ApJ*, 532, 1111 (HTBK)
- Hamaguchi, K., Yamauchi, S., & Koyama, K. 2005, *ApJ*, 618, 360
- Herbig, G. H. 1960, *ApJS*, 4, 337
- Hillenbrand, L. A., Strom, S. E., Vrba, F. J., & Keene, J. 1992, *ApJ*, 397, 613
- Hubrig, S., Schöller, M., & Yudin, R. V. 2004, *A&A*, 428, L1
- Pogodin, M. A., Miroshnichenko, A. S., Tarasov, A. E., et al. 2004, *A&A*, 417, 715
- Praderie, F., Catala, C., Simon, T., & Boesgaard, A. M. 1986, *ApJ*, 303, 311
- Rieke, G. H., & Lebofsky, M. J. 1985, *ApJ*, 288, 618
- Siess, L., Dufour, E., & Forestini, M. 2000, *A&A*, 358, 593
- Skinner, S. L., & Yamauchi, S. 1996, *ApJ*, 471, 987
- Skinner, S. L., Güdel, M., Audard, M., & Smith, K. 2004, *ApJ*, 614, 221
- Smith, K. W., Balega, Y. Y., Duschl, W. J., et al. 2005, *A&A*, 431, 307
- Testi, L., Palla, F., & Natta, A. 1998, *A&AS*, 133, 81
- Testi, L., Palla, F., & Natta, A. 1999, *A&A*, 342, 515
- Tsuboi, Y., Koyama, K., Murakami, H., et al. 1998, *ApJ*, 503, 894
- van den Ancker, M. E., The, P. S., Tjin A Djie, H. R. E., et al. 1997, *A&A*, 324, L33
- Vink, J. S., O'Neill, P. M., Els, S. G., & Drew, J. E. 2005, *A&A*, 438, L21
- Wolk, S. J., Harnden, F. R., Flaccomio, E., et al. 2005, *ApJS*, 160, 423